TRI-PP-85-24
Apr 1985

A MULTI ANODE PHOTOMULTIPLIER WITH POSITION SENSITIVITY

M. Salomon and S.S.A. Williams
TRIUMF, 4004 Wesbrook Mall, Vancouver, B.C. V6T 2A3 Canada

Abstract

We have measured the properties of a specially developed photomultiplier with proximity dynodes and 10 wire anodes. This design allows us to determine the position of emission of the photoelectrons from the cathode with an accuracy of 1.3 mm FWHM. This tube is also extremely fast due to the short transit time and the geometry of its dynodes.

(Submitted to Nuclear Instruments & Methods)

1. Introduction

The objective of this study has been to test a multi-anode photomultiplier in order to determine its possible use as a position sensitive detector for a Positron Emission Tomograph (PET) camera and other applications in particle physics. Apart from position sensitivity, we therefore needed a detector with fast time response, high gain and high dynamic range.

At the present time, PET cameras use an array of optically separated scintillators, each coupled to its own photomultiplier (PMT). The development of a position sensitive PMT would make the camera much less expensive and more accurate due to the fact that fewer photomultipliers would be required.

While motivation for testing this device derives from the PET camera application, it would have more general applications as a one dimensional position sensitive detector for hodoscopes, fiber scintillators and other devices. This report describes the design and basic characteristics of such a PMT.

Previous designs of position sensitive photomultipliers include [1] a prototype multianode PMT incorporating a chevron type multichannel plate (MCP) electron multiplier and 400 multi anodes. This tube achieved a 0.6 mm spatial resolution over the anode surface and about 600 ps rise time in the output signal. This design however, had several drawbacks such as large dark current which makes single photon counting difficult, a saturation effect which limits the counting rate of pulses and a short life time of the MCP. These effects can be reduced but not eliminated. Another PMT was designed with multistage focussing dynodes [2] and divided anode and used localization of secondary electrons by means of an axial magnetic field. The PMT had a gain of 10^5 to 10^6 for 10 dynodes, and an intrinsic resolution of about 3.4 mm in both x and y directions. A PMT with fine mesh dynodes [3] and resistive anode was also designed. The resistive anode consisted of KCsSb instead of the usual metal oxide film which is unstable during the tube processing. This PMT had a spatial resolution of 4.2 mm for scintillation imaging with ^{137}Cs. Finally, ITL [4] manufactured an imaging photon detector which incorporates a resistive anode with 4 electrodes to produce two dimensional imaging. This device is capable of detecting extremely weak signals and has a resolution of 10 lines/mm. Several other types of imaging devices are now manufactured commercially but use multichannel plates instead of dynodes.

2. Structure of photomultiplier

The PMT tested was built by Hamamatsu, and is a modified version of the Hamamatsu R1652. It has 9 fine mesh dynodes and a proximity construction between the photocathode and the first dynode [3]. The structure of the tube, as well as its overall dimensions, is shown in fig. 1. Fig. 1(a), shows the 9 stages of mesh dynode which are followed by a linear array of 10 multi anodes and a last reflective dynode. The 10 anodes are spaced about 5 mm apart and are 5 cm long. Fig. 1(b), shows the anode wires in front of the last dynode.

3. Energy resolution

We tested the PM energy resolution by adding the signals of all anodes and integrating them over 400 ns. The resistive chain used to bias the dynodes had 10 stages of 100 KΩ each in order to obtain maximum gain. It drew a current of 1.5 mA at 1500 volts. The last 4 stages had decoupling capacitors. The resistive load at each anode was 10 KΩ. An

electrostatic shielding surrounded the tube and was connected to the photocathode through a 10 MΩ resistor. We operated the tube with a negative high voltage. The gain at 1500 V was approximately 10^4 when adding all anode signals. The source was ^{60}Co and the scintillator a 5.1 cm diameter and 5.1 cm long cylinder of NaI(Tℓ). The FWHM of the 1.17 and 1.33 MeV gamma ray peaks was 9% and 8% respectively.

These results are comparable to standard photomultipliers, indicating that the cathode photoefficiency is larger than 15% and that the PM can be used in low light level applications as would be the case in PET machines or with fiber scintillators.

One source of resolution degradation is the uncertainty of multiplication in the last dynode. Some electrons originating in dynode 9 will be collected by the anode wires, while others will be further multiplied in the reflecting dynode 10. This effect does not seem very large, as the energy resolution is comparable to normal phototubes, presumably because only a small fraction of the electrons of dynode 9 are collected by the anodes.

4. Response to point light sources

In order to test the position response of the PMT it was first necessary to find a light source that was both narrow and capable of being moved across the front of the photomultiplier. This was accomplished with a collimated ^{106}Ru source and a 1 mm thin NE102 plastic scintillator. The scintillator was mounted over a hole 0.8 mm diameter in a lead collimator and the source was mounted on a calliper which enabled it to be moved in front of the PMT with an accuracy and reproducibility of 0.3 mm. The source was oriented in such a way that it moved perpendicular to the wire anodes. This geometry is shown in fig. 2.

Measurements were made of the magnitude of the charge Q_i collected at each anode, with respect to the position of the source in front of the PMT. A plot of these measurements is shown in fig. 3. These data show that the electron shower extends approximately 14 mm FWHM for each anode.

5. Position information

When the source is at any one position in front of the PMT, the photocathode produces electrons which after multiplication appear at only a few of the anodes. This observation leads to the conclusion that by measuring the relative charge at each anode one can determine the position of the source. The arrangement used for measuring the charge at each anode is shown in figs. 2 and 4.

A scintillation event from the source results in a net charge at the anodes that is higher than the background or noise level of the PMT. This causes the discriminator to trigger the computer, which reads the ADC's (LRS2249W) corresponding to each anode. The values read by the computer are directly proportional to the charge at each anode. The discriminator level was set at approximately 10^4 electrons. The gate pulse for the ADC was 40 ns.

As a first approximation, the position of the source was calculated from the center of gravity equation:

$$G_1 = \sum_{i=2}^{8} X_i C_i Q_i / \sum_{i=2}^{8} C_i Q_i \qquad (1)$$

The subscript i corresponds to the number assigned to each anode. In this test only 7 of the photomultiplier's 10 anodes were used. X_i, is a constant proportional to the position of each anode and C_i, is a normalization factor which corrects for the non uniformity of charge

gain at each anode. This non uniformity of charge can be seen as the different peak heights in the plot of fig. 3. Finally, Q_i, is the charge at each anode as measured by the ADC.

Fig. 5, shows the computer generated histogram of G_1, calculated from eq. (1), with the source at 3 different positions. This yields a position resolution of 1.8 mm FWHM.

A second equation for source position was used to reduce the effect of the tails of the anodes charge distribution. This equation is as follows:

$$G_2 = \sum_{i=2}^{8} X_i (C_i Q_i)^2 / \sum_{i=2}^{8} (C_i Q_i)^2 \ . \qquad (2)$$

The histogram for G_2, using this new equation is shown in fig. 6. The peak has a resolution of 1.3 mm FWHM with the source at 3 different positions. This resolution is close to the expected limit due to the finite size of the source.

The mean value of G_2 from (2), is plotted as a function of the actual source position in fig. 7. The data shows that within a region of 3 cm of the center of the PMT, the relationship between the calculated position and the actual source position is linear. The non-linearity outside this region is due to the fact that only 7 anodes were used in this measurement. The linear region can be extended to 5 cm with the use of all anodes.

We also studied the effect of the signal size on the spatial resolution by measuring the FWHM of the peaks as a function of the discriminator level (CFD) shown in fig. 4. This result is shown in fig. 8, and indicates an optimum value of discrimination below which the position information deteriorates. This value corresponds to approximately

300 keV photons in a plastic scintillator or 60 keV in a NaI(Tℓ) scintillator.

7. Timing response

The system used for measuring the timing response of the R1652 consisted of a pulsed light source (xenon flash lamp) optically coupled to the PMT by a thin (1 mm diameter) fiber optic cable. This arrangement is favourable because the light source is narrow and allows variable intensity, frequency and position.

When the xenon flash lamp was triggered it produced a light pulse of about 200 ns in length with a very short rise time and a 50 ns exponential decay. This pulse was sent through the fiber optics to two photomultipliers. An RCA 8575 PMT was used to trigger the computer and the time delay between the RCA signal and the R1652 signal was measured in a TDC. This quantity was then histogrammed by the computer.

The transit timing response of the R1652 was measured as a function of the voltage applied to the PMT. A plot of transit time versus applied voltage is shown in fig. 9. This measurement was made with all 10 anodes summed to produce the stop pulse. Fig. 10, shows the computer generated histogram for the time between the START and STOP pulses with an applied voltage of 1400 V. The time resolution was 550 ps FWHM at a voltage of 1400 V.

We also tested the timing response with source position when the STOP signal was supplied by only one anode. The fiber-optic cable was moved across the front of the PMT and timing measurements were made for several different positions. Fig. 11, shows the time vs position plot for anode 6 and 7. The minimum in this peak corresponds to the position where the light source is directly in front of the corresponding anode

wire. By using a constant fraction discriminator the effect of changing signal amplitudes was minimized.

8. Summary and conclusions

The Hamamatsu R1652 with linear anode array showed good position sensitivity. The PMT was able to produce a position resolution of 1.3 mm, which includes the source width of 1.0 mm, and a time resolution of 550 ps FWHM. The PMT appears to be suitable for one dimensional, position sensitive photon detection and could be adapted for use with imaging cameras. One drawback with this PMT is that it only has one dimensional position sensitivity. This can be obviated with pads as anodes or using resistive cathodes. Resistive cathodes however, have the disadvantage of ambiguous response for multiple events and a large array of pads requires a very large number of pins on the tube. Therefore the final design for tubes of this kind have to be tailored to the particular experiment or application.

References

[1] K. Oba, et al., IEEE Trans. Nucl. Sci. Vol. NS-26 (1979) 346.

[2] J. Ditta et al., Nucl. Instr. and Methods, 220 (1984) 343 and reference therein.

[3] H. Kume, S. Suzuki, J. Takeuchi, K. Oba, IEEE Trans. Nucl. Sci., Vol. NS-32 (1985) 355 and NS-32 (1985) 448.

[4] Report from: Instrument Technology Ltd., Imaging photon detector. St. Leonards-on-Sea, East Sussex, U.K.

Figure Captions

1a. Mechanical side view of the photomultiplier showing the photocathode, followed by 9 dynodes, the array of 10 anodes and the reflecting last dynode. (All dimensions in millimeters).

1b. Mechanical front view of the anode wires and the reflecting last dynode.

2. Layout of a movable source and scintillator to test the position resolution of the photomultiplier. The scintillator thickness was 1 mm and the height 10 mm. The position accuracy of the source and scintillator was 0.3 mm.

3. The charge collected on each anode (arbitrary scale) as a function of the source position. The center of the photomultiplier corresponds approximately to position 140 mm.

4. Electronic diagrams used in the position measurements. The amplifiers had a gain of 10, the gate length at the ADC was 40 ns and the event rate was 10^2 per second.

5. Result of the center of gravity method described in the text, where G_1 is the first moment of the normalized anode signals. The 3 peaks correspond to 3 positions of the source.

6. Result of the center of gravity method using a second moment G_2 for the normalized anode signals. The 3 peaks correspond to 3 positions of the source.

7. The average values of G_2 for 8 different positions of the source, as a function of their actual position. This curve indicates the linear region for this algorithm. This region can be extended however, by modifying the normalization coefficients C_i described in the text.

8. The position resolution, measured as the ratio of the standard deviation and the average of G, as a function of the threshold in the Constant Fraction Discriminator.

9. The electron transit time as a function of the applied voltage on the photomultiplier. We used the value of 15 ns at 1250 V measured by the manufacturers as our delay calibration.

10. The timing resolution measured with 3 relative delays using a light flash tube (Xenon) and a second photomultiplier as a reference.

11. The variation of electron transit time with the position of the light source. We used a 1 mm diameter light fiber attached to the calibrated displacement used in the position measurements.

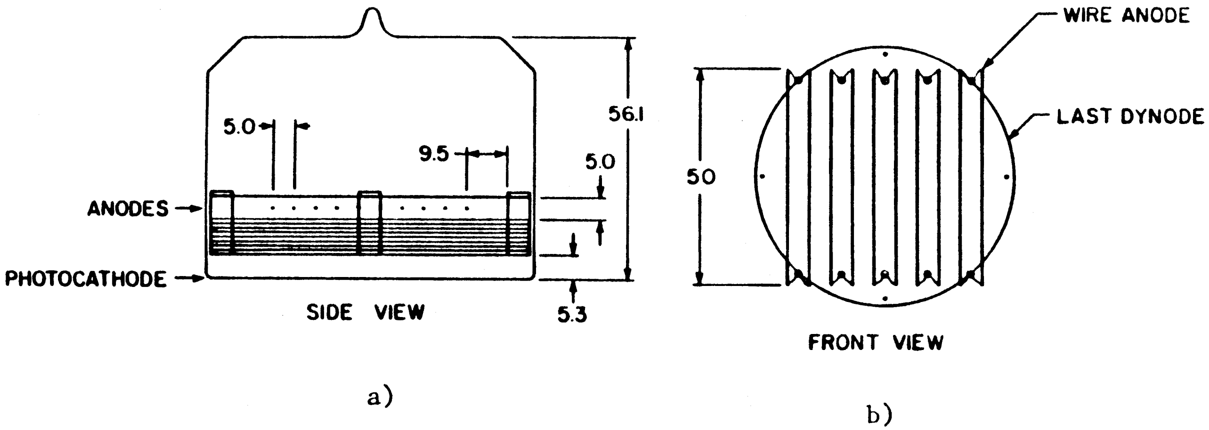

Fig. 1

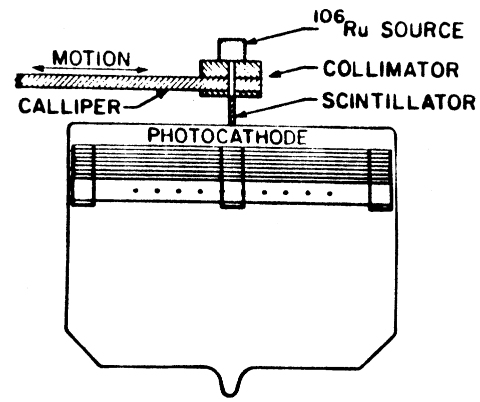

Fig. 2

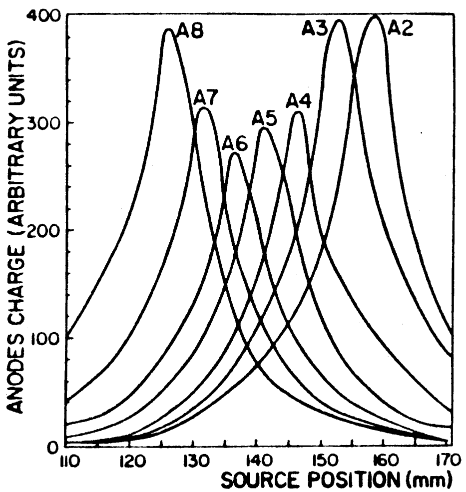

Fig. 3

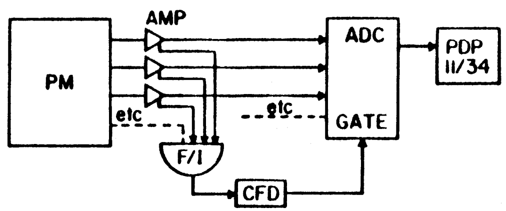

Fig. 4

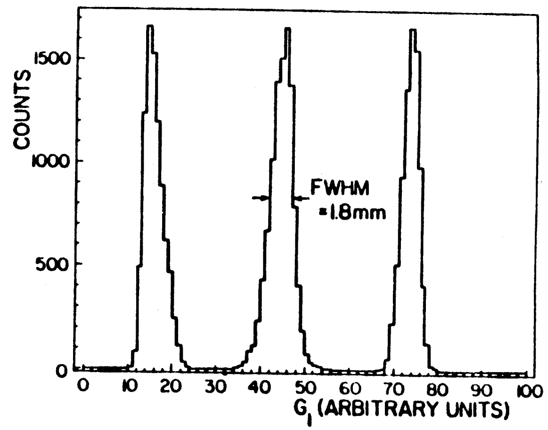

Fig. 5

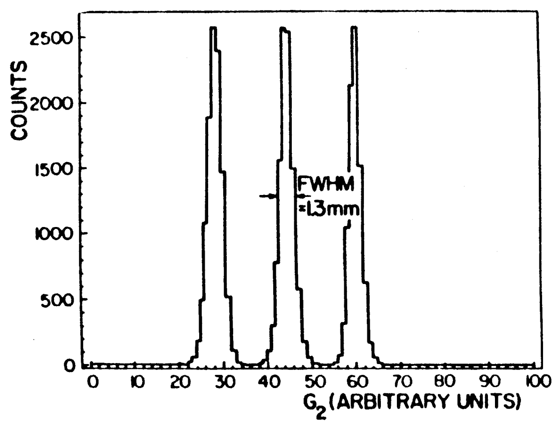

Fig. 6

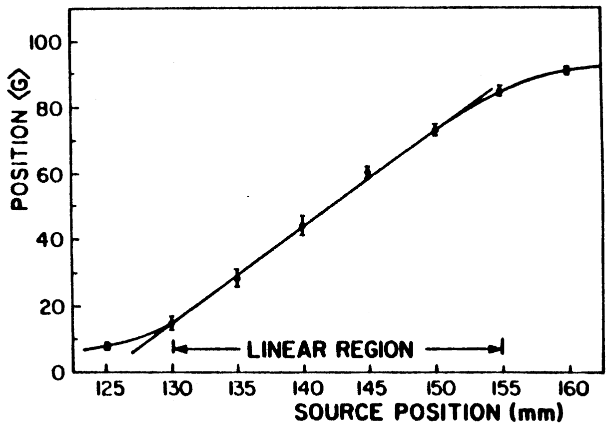

Fig. 7

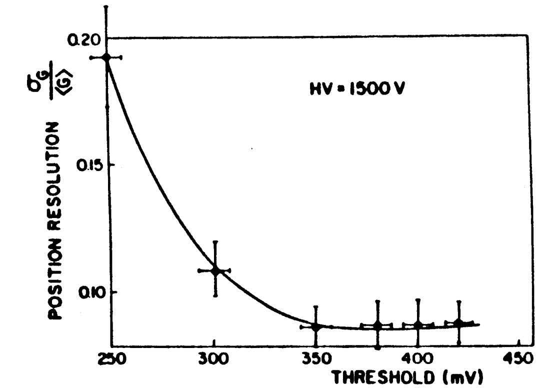

Fig. 8

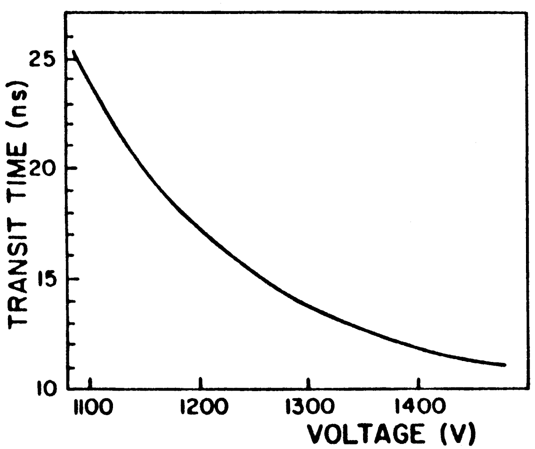

Fig. 9

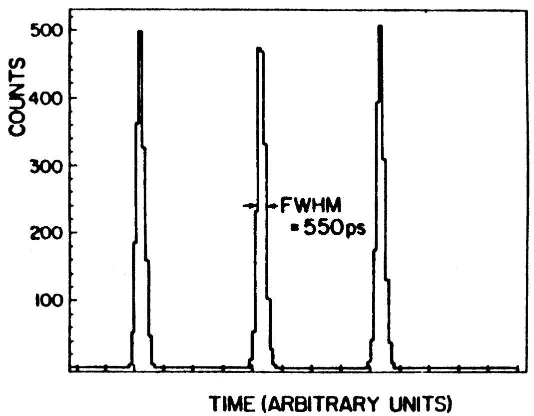

Fig. 10

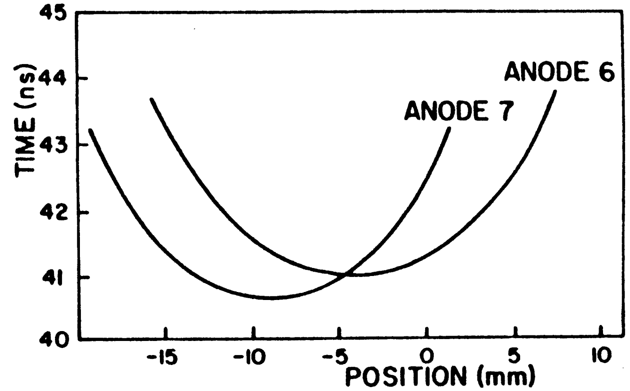

Fig. 11